Hindawi Publishing Corporation
Journal of Nanomaterials
Volume 2013, Article ID 497318, 8 pages
http://dx.doi.org/10.1155/2013/497318

Research Article

Flame-Made Pt-Loaded TiO_2 Thin Films and Their Application as H_2 Gas Sensors

Weerasak Chomkitichai,[1] Hathaithip Ninsonthi,[1] Chaikarn Liewhiran,[2] Anurat Wisitsoraat,[3] Saengrawee Sriwichai,[1] and Sukon Phanichphant[4]

[1] *Department of Chemistry, Faculty of Science, Chiang Mai University, 239 Huay Kaew Road, Muang District, Chiang Mai 50200, Thailand*
[2] *Department of Physics and Materials Science, Faculty of Science, Chiang Mai University, 239 Huay Kaew Road, Muang District, Chiang Mai 50200, Thailand*
[3] *Nanoelectronics and MEMS Laboratory, National Electronics and Computer Technology Center, Klong Luang, Pathumthani 12120, Thailand*
[4] *Materials Science Research Center, Faculty of Science, Chiang Mai University, 239 Huay Kaew Road, Muang District, Chiang Mai 50200, Thailand*

Correspondence should be addressed to Sukon Phanichphant; sphanichphant@yahoo.com

Received 10 August 2013; Revised 24 October 2013; Accepted 4 November 2013

Academic Editor: Sheng-Joue Young

The hydrogen gas sensors were developed successfully using flame-made platinum-loaded titanium dioxide (Pt-loaded TiO_2) nanoparticles as the sensing materials. Pt-loaded TiO_2 thin films were prepared by spin-coating technique onto Al_2O_3 substrates interdigitated with Au electrodes. Structural and gas-sensing characteristics were examined by using scanning electron microscopy (SEM) and showed surface morphology of the deposited film. X-ray diffraction (XRD) patterns can be confirmed to be the anatase and rutile phases of TiO_2. High-resolution transmission electron microscopy (HRTEM) showed that Pt nanoparticles deposited on larger TiO_2 nanoparticles. TiO_2 films loaded with Pt nanoparticles were used as conductometric sensors for the detection of H_2. The gas sensing of H_2 was studied at the operating temperatures of 300, 350, and 400°C in dry air. It was found that 2.00 mol% Pt-loaded TiO_2 sensing films showed higher response towards H_2 gas than the unloaded film. In addition, the responses of Pt-loaded TiO_2 films at all operating temperatures were higher than that of unloaded TiO_2 film. The response increased and the response time decreased with increasing of H_2 concentrations.

1. Introduction

Metal oxide nanopowders offer promising research materials because of their wide range of applications. Many studies have focused on enhancing the performance of gas sensors. They were synthesized by different techniques such as the modified sol-gel method [1], thermal plasma [2], hydrothermal [3], and flame spray pyrolysis [4, 5]. Flame spray pyrolysis (FSP) is one-step synthesis method that is suitable for large-scale production of noble metal-metal oxide nanocomposites [6–8].

Hydrogen gas is an important gas for clean energy sources, highly flammable, and burnable in air at a very wide range (4–75% by volume) [9–11]. However, its presence due to leakage at a sufficient high concentration together with oxygen in air will cause explosion. Moreover, H_2 cannot be detected by human senses when it leaks. Therefore, semiconducting Pt-loaded TiO_2 is one of the most promising candidates for flammable gas detection due to its advantages including low cost, high sensitivity, fast response, simplicity of use, and ability to detect a large number of gases.

In this study, we report the synthesis of unloaded TiO_2 and Pt-loaded TiO_2 by FSP and study the effect of Pt catalyst dispersion in TiO_2 nanopowder surface on hydrogen gas-sensing behaviors due to the fact that Pt nanoparticles dispersed on the TiO_2 surface can act as electron sinks and result in a decrease in electron-hole recombination [12]. In addition, Pt is known to be a very effective catalyst for several reducing gases on metal oxide supports [13, 14].

2. Experimental

FSP process was operated to produce the flame-spray-made unloaded TiO_2 and Pt-loaded TiO_2 nanopowders. Precursor solutions (0.50 M) were prepared by dissolving appropriate amounts of titanium isopropoxide (Aldrich, 97%) and platinum (II) acetylacetonate (Aldrich, 97%) dissolved in xylene (Carlo Erba, 98.5%). The loading concentrations in mol% fraction of Pt were set as 0.25%, 0.50%, 0.75%, 1.00%, 2.00%, and 3.00%. The unloaded TiO_2 and Pt-loaded TiO_2 nanopowders synthesized by FSP were also previously reported by other studies [4, 9].

The crystallinity phases of unloaded TiO_2 and Pt-loaded TiO_2 were analyzed by X-ray diffraction (XRD, Philips X' Pert MPD) using CuKα radiation at 2θ = 20–80° with a scanning speed of 5°/min. The morphology and size of the nanoparticles were characterized by scanning electron microscopy (SEM) and high-resolution transmission electron microscopy (HR-TEM). The existence of Pt was confirmed by energy-dispersive X-ray spectroscopy (EDS).

The unloaded TiO_2 and Pt-loaded TiO_2 sensing films were fabricated according to a previous report [9]. The gas-sensing characteristics of unloaded TiO_2 and Pt-loaded TiO_2 sensing films in a stainless steel chamber were characterized over a high-concentration range of H_2 gas (150–10,000 ppm). The standard flow through technique was used to test the gas-sensing properties of unloaded TiO_2 and Pt-loaded TiO_2 films. A constant flux of synthetic air of 2 L/min as gas carrier was flowed to mix with the desired concentration of hydrogen gas dispersed in synthetic air. The sensors were tested for hydrogen gas at the operating temperature of 300–400°C. It should be noted that the operating temperature could not be below 300°C since the resistances of Pt-loaded TiO_2 films were too high and could not be measured below 300°C. By monitoring the output current through the sensor, the resistances of the sensor were continuously recorded to evaluate the sensor response, response time and recovery time. The sensor response (S) is defined as the resistance ratio R_a/R_g (R_a is a resistance in dry air, R_g is a resistance in the test gas) [9]. Response time is defined as the time required until 90% of the response signal is reached while recovery time is the time to recover to 90% of baseline resistance.

3. Results and Discussion

3.1. Particle and Sensing Films Properties. The XRD spectra of unloaded TiO_2 and 0.25, 0.50, 0.75, 1.00, 2.00, and 3.00 mol% Pt-loaded TiO_2 nanopowders are shown in Figure 1. The diffraction peaks of the unloaded TiO_2 and Pt-loaded TiO_2 samples showed that both anatase and rutile phases in the seven samples are very similar, which matched well with the *JCPDS file no. 21-1272 and =JCPDS file no. 21-1276, respectively. The XRD peak of Pt peaks was not found in these patterns (JCPDS file no. 87-0640) because Pt was loaded in the range of very low concentration when comparing with the TiO_2 nanoparticles [8, 9, 15].

The bright-field TEM imaging was used to investigate the 2D accurate size and morphology of the nanopowders as

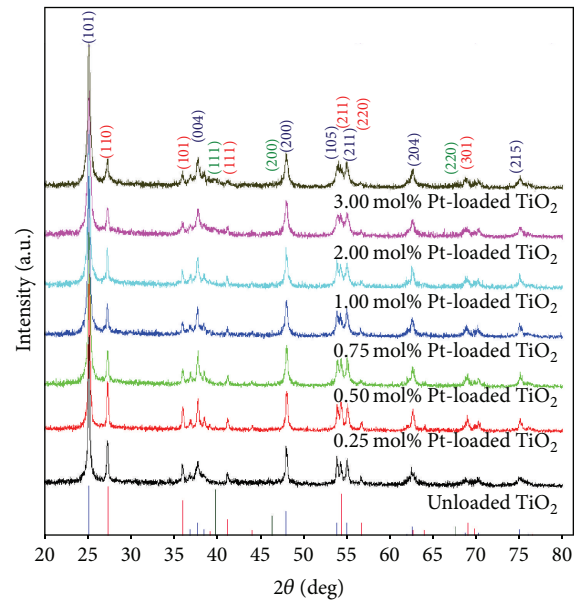

*JCPDS number of TiO_2 = 21-1272 (anatase)
*JCPDS number of TiO_2 = 21-1276 (rutile)
JCPDS number of Pt = 87-0640

Figure 1: XRD patterns of flame-made (5/5) unloaded TiO_2 and Pt-loaded TiO_2 nanoparticles.

shown in Figure 2. The presence of TiO_2 spherical nanoparticles along with smaller Pt nanoparticles (dark spots) confined on the TiO_2 surface was observed as shown in Figures 2(a) and 2(b). The crystallite sizes of spherical particles were found to be ranging from 5 to 40 nm whereas the average diameter of Pt nanoparticles was about 2 nm. The selected area electron diffraction (SAED) patterns of unloaded TiO_2 and 2.00 mol% Pt-loaded TiO_2 in Figures 2(a) and 2(b) were indexed and identified as the crystal structure, corresponding to the (101), (004), (200), and (105) crystal planes of anatase phases of unloaded TiO_2 and 2.00 mol% Pt-loaded TiO_2. The SAED rutile of TiO_2 was not detected possibly because the ratio of anatase and rutile is significantly different. Figure 2(c) shows lattice fringes of TiO_2 sample. The lattice fringes of TiO_2, matching well with d-spacing of TiO_2, were measured and identified as the crystal structure of TiO_2. The dominance of (004) and (200) planes of anatase and (110) planes of rutile structure can be used to confirm the fringe widths of 0.231 nm, 0.180 nm, and 0.245 nm, respectively.

The surface morphology of highly crystalline 0.50 mol% Pt-loaded TiO_2 nanoparticles for SEM analysis and EDS spectrum is shown in Figures 3(a) and 3(b), respectively. It illustrates that the film surface is highly porous and contains high-density nanoparticles. The EDS analyses show the presence of Pt, Ti, and O as part of composition of the material. The cross-sectional SEM micrograph of 0.50 mol% Pt-loaded TiO_2 thin film onto Al_2O_3 substrate interdigitated with Au electrodes after annealing and sensing test at 300°C, 350°C, and 400°C in dry air is shown in Figure 3(c), showing that the thickness of sensing film is approximately 15 μm (side view).

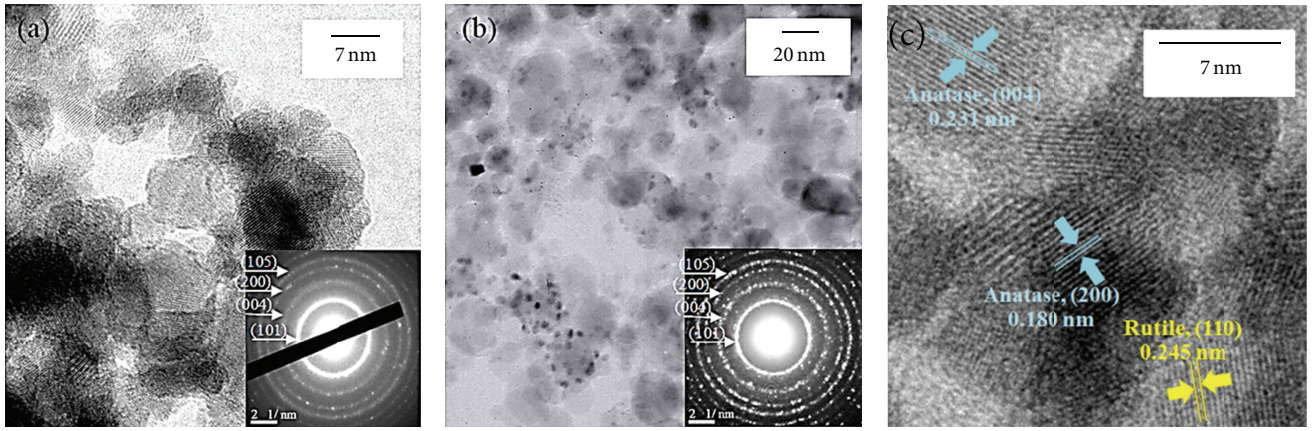

(a) (b) (c)

Figure 2: HRTEM and SAED images of (a) unloaded TiO_2, (b) 2.00 mol% Pt-loaded TiO_2 nanoparticle sizes and (c) lattice fringes image of TiO_2.

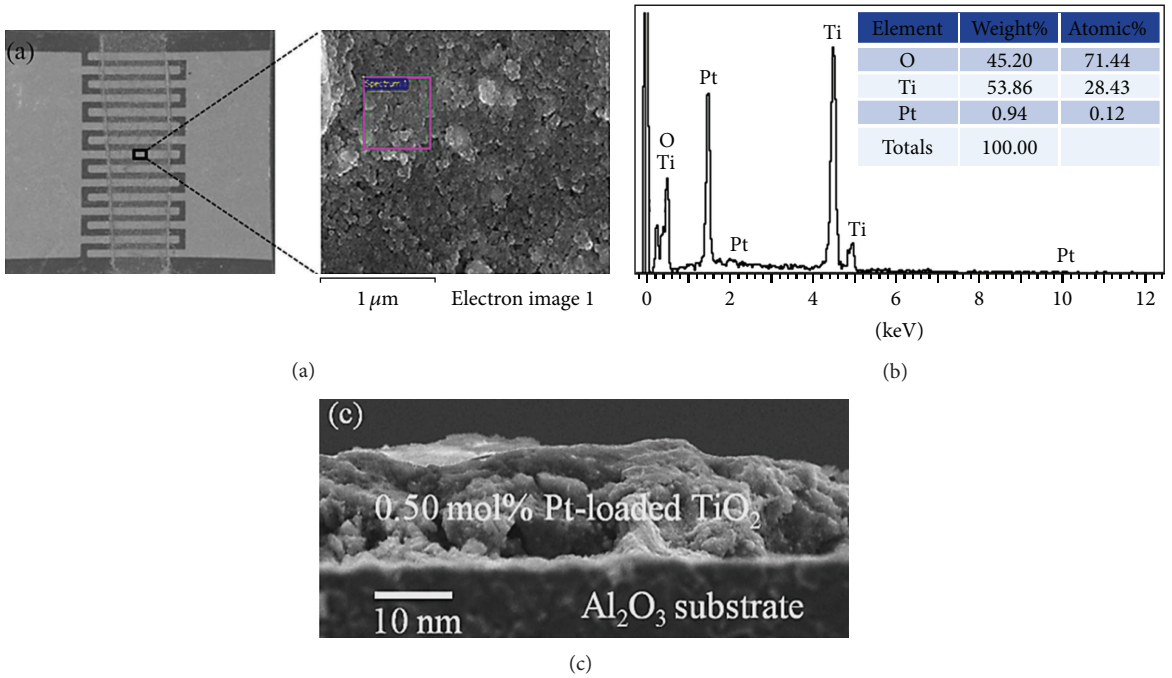

(a) (b)

(c)

Figure 3: (a) SEM image and (b) corresponding selected area-EDS analysis of the flame-made (5/5) 0.50 mol% Pt-loaded TiO_2 films sensor on an Al_2O_3 substrate interdigitated with Au electrodes. (c) The cross-sectional sensing films were spin-coated onto Au/Al_2O_3 substrate after annealing and sensing test at 300–400°C in dry air.

3.2. Hydrogen Gas-Sensing Properties. The interaction of the resistive sensors with analyzing H_2 gas caused a change in the resistance of the unloaded TiO_2 and Pt-loaded TiO_2 sensors. Figure 4(a) shows the sensor resistance versus sensing time of H_2 sensing characteristics performed at the operating temperature of 300°C with different H_2 gas concentrations (0.015–1 vol%) and Pt loading levels (0–3.00 mol%). The interaction of the resistive sensors with a target gas resulted in a change in electrical conductance upon the gas exposure. The original baseline in resistance was quite stable after recovering from multiple gas exposures. When a reducing gas was detected using *n*-type semiconductors (TiO_2), the resistance decreased due to the increased number of electrons on the semiconductor surface [16]. In addition, the resistance change was enhanced significantly with Pt loading and was monotonically increased with gas concentration. The sensing behaviors were subsequently analyzed in terms of sensor response (*S*), response time, and recovery time as illustrated in Figures 4(b), 4(c), and 4(d), respectively. The sensor response greatly increased with increasing Pt loading level

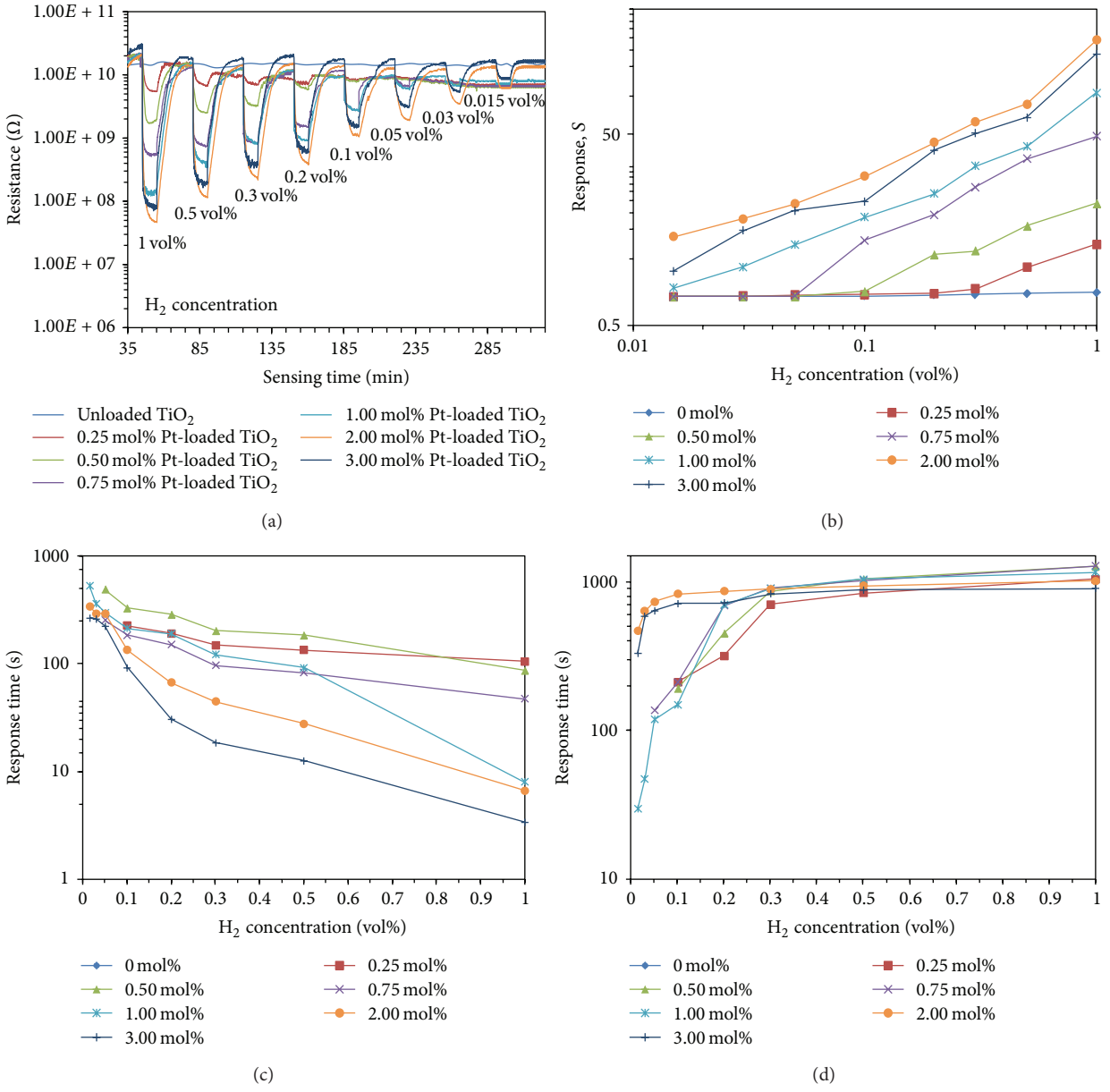

Figure 4: (a) Change in resistance, (b) the sensor response, (c) response time, and (d) recovery time of unloaded TiO_2 and Pt-loaded TiO_2 sensors upon exposure to H_2 at operating temperature of 300°C.

up to 2.00 mol% but decreased as the loading level increased further to 3.00 mol% at all gas concentrations. In addition, the sensor response increased linearly in log-log scale, indicating that the hydrogen response followed the well-known power law.

The hydrogen detection limits at 300°C of Pt-loaded TiO_2 sensors were then estimated by power-law fitting the response curve and calculating the concentration at which the response was 1.1 (10% change of resistance). The calculated detection limits of unloaded and 0.25, 0.5, 0.75, 1.00, 2.00, and 3.00 mol% Pt-loaded TiO_2 sensors were estimated to be 1, 0.3, 0.1 and 0.05, 0.013, 0.004, and 0.009 vol%, respectively. The detection limits of TiO_2 sensors were greatly improved with Pt loading and the 2.00 mol% Pt-loaded TiO_2 sensor exhibited a low detection limit of 40 ppm, which can potentially be used for hydrogen leak detection.

In terms of response time (Figure 4(c)), the response time decreased rapidly with increasing H_2 concentration and was substantially improved with increasing Pt loading level. The response time naturally decreased with gas concentration due to faster gas dynamic at high concentration while Pt reduced the response time via catalytic effect, in which the hydrogen was quickly dissociated by Pt nanoparticles. The reaction rate monotonically increased with amount of Pt as 3.00 mol% Pt resulted in shorter response time than 2.00 mol% Pt. The 2.00 and 3.00 mol% Pt-loaded TiO_2 sensors exhibited very short

response times of ~8 and ~5 seconds at H_2 concentration of 1 vol%. Regarding the recovery time (Figure 4(d)), the recovery time increased relatively slowly with increasing H_2 concentration and was rather insensitive to Pt loading level. The recovery time naturally increased with gas concentration due to longer time required to desorb larger amount of adsorbed gas species at high concentration while Pt does not play a direct role in desorption of hydrogen. The Pt-loaded TiO_2 sensors require rather long recovery time in the range of 700–1000 seconds, which could be due to longer time required for gas to diffuse out of the thick and porous TiO_2 layer.

Operating temperature generally has an important impact on the performance of semiconductor gas sensors. Typically, the sensing response of the metal oxides tends to increase with increasing temperature [17, 18]. Figure 5 shows the electrical resistance in air of 2.00 mol% Pt-loaded TiO_2 thick-film sensor as a function of time at different temperatures of 300°C, 350°C, and 400°C for the thick films of 2.00 mol% Pt-loaded TiO_2. It was shown that the baseline resistance of the Pt-loaded sensor tends to decrease with increasing operating temperature while the resistances under 1 vol% hydrogen exposure are quite similar. Thus, the resistance change and corresponding response are decreased with increasing operating temperature. The effects of Pt loading level and operating temperature on gas-sensing response of 1 vol% H_2 performed at 300–400°C are shown in Figure 6. Pt-loaded TiO_2 sensors exhibited relatively high responses at 300°C and the response at the optimal operating temperature was particularly pronounced at 2.00 mol% Pt loading concentration. At higher operating temperature (350–400°C), Pt loading provided relatively lower enhancement of sensor response. Thus, the suitable operating temperature and concentration of Pt loading can greatly improve H_2 response of TiO_2 sensors. The best sensing performance with a high sensor response to 1 vol% of H_2 concentration of 470 was obtained at the optimal Pt-loading level of 2.00 mol% and optimal operating temperature of 300°C.

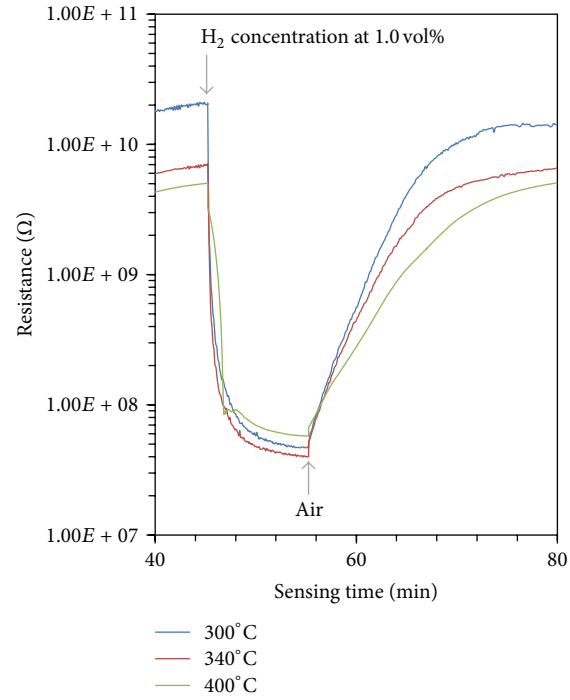

Figure 5: Electrical resistance change induced at 300°C, 350°C, and 400°C for the thick films of 2.00 mol% Pt-loaded TiO_2.

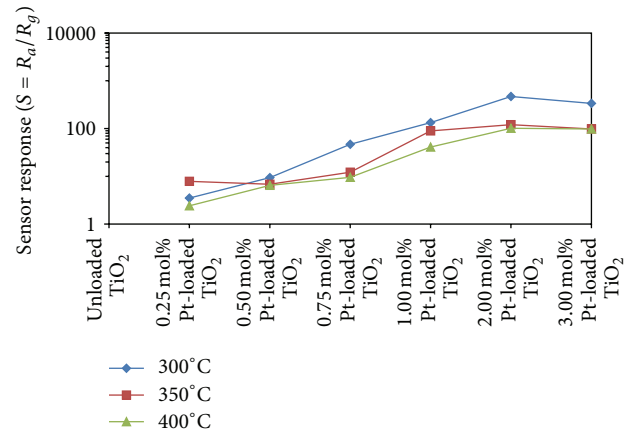

Figure 6: Variation of the sensor response to 1 vol% of H_2 with different operating temperatures ranging from 300 to 400°C.

3.3. Hydrogen Gas-Sensing Mechanisms. From experimental results, unloaded TiO_2 sensor exhibited very low response to H_2 at operating temperatures 300–400°C, which is in accordance with other reports indicating that direct dissociation of hydrogen on metal oxides will be effective above 400°C [19]. With Pt loading in the range between 0.25 and 3.00 mol%, hydrogen response increased substantially. It has been widely accepted that Pt enhances sensitivity and response rate of a metal oxide sensor via chemical sensitization with hydrogen gas. Pt can dissociate H_2 into H atoms, which interact with TiO_2 support via the *spillover* process according to the reaction [20]:

$$H_2 \longrightarrow 2H_{ad} \quad (1)$$

The adsorbed hydrogen molecules will interact with the preadsorbed oxygen species including O_2^-, O^-, and O^{2-}, which were thermally activated on Pt-loaded TiO_2 surface, according to [21–24]:

$$4H_{ad} + O_{2\,(ad)}^- \longrightarrow 2H_2O_{(des)} + e^- \quad (2)$$

$$2H_{ad} + O_{(ad)}^- \longrightarrow H_2O_{(des)} + e^- \quad (3)$$

$$2H_{ad} + O_{2\,(ad)}^- \longrightarrow H_2O_{(des)} + 2e^- \quad (4)$$

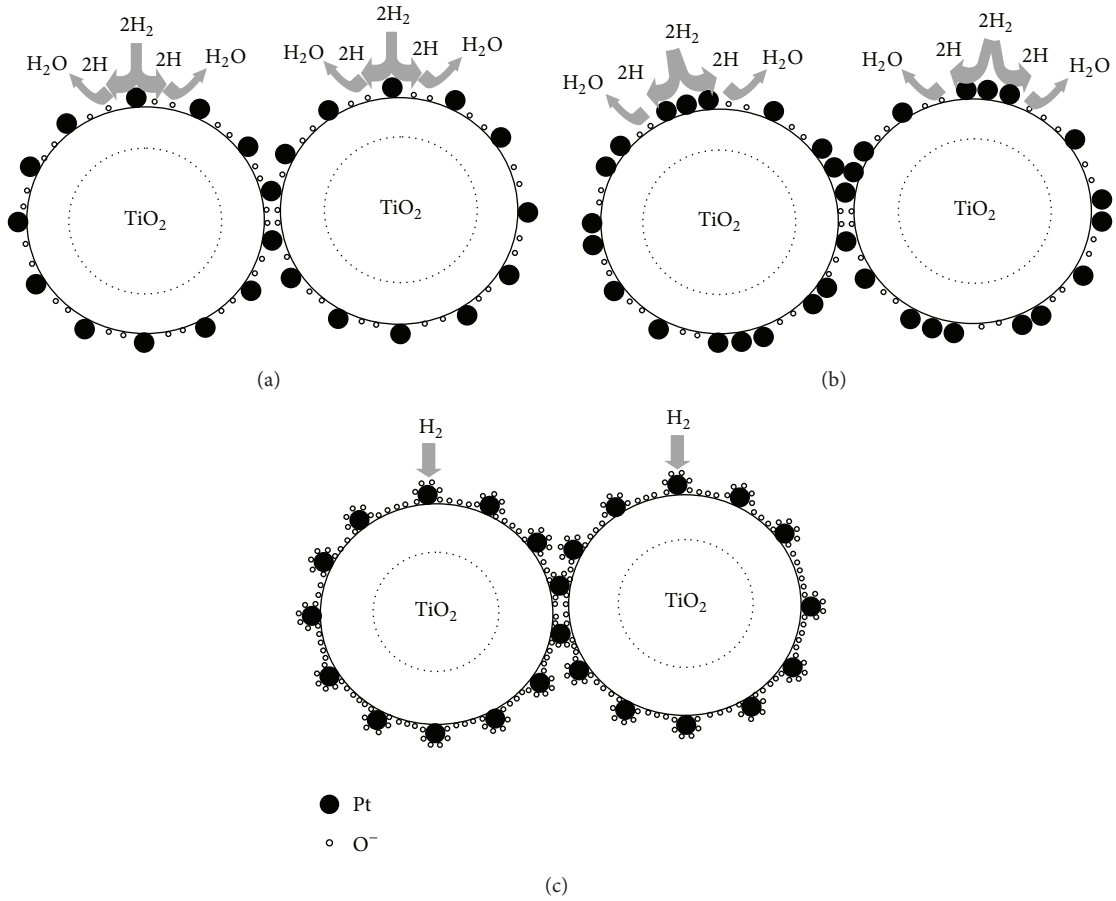

Figure 7: Schematic gas-sensing mechanisms of Pt-loaded TiO_2 nanoparticles with (a) optimal Pt concentration (2.00 mol%) and (b) excessive Pt concentration (3.00 mol%) at low operating temperature (300°C) and (c) with optimal Pt concentration at high operating temperature (350–400°C).

These reactions produce more electrons and thus increase the conductivity of *n*-type semiconductor (TiO_2) upon exposure to hydrogen with preadsorbed oxygen which leads to freeing of previously trapped electrons.

In order for the catalyst to be effective, there must be a good dispersion and appropriate amount of the catalysts; thus, catalyst particles are available near most interparticle contacts as illustrated in Figure 7(a). The spillover species must be able to migrate to most interparticle contacts in order to dominate the metal oxide resistance. The spillover mechanism will become less effective when catalyst particles are agglomerated or poorly dispersed as depicted in Figure 7(b). The agglomeration and poor dispersion of Pt nanoparticles reduce the number of spillover hydrogen species on TiO_2 support, thereby reducing the hydrogen response. Such aggregation is highly likely when the Pt loading concentration increases to a level as high as 3.00 mol%. Thus, 2.00 mol% is the optimal Pt loading level that yields high amount of Pt with good dispersion on FSP-made TiO_2 nanoparticle supports, which results in an optimal hydrogen response.

For the effect of operating temperature, Pt-loaded TiO_2 films exhibited optimum hydrogen response at temperature of 300°C and higher operating temperature leads to considerably degraded response. An explanation of sensor response of the temperature-induced change may be formulated by considering the occurrence of different types and concentrations of ionosorbed surface reactive oxygen species (O_2^-, O^-, or O^{2-}) on the Pt-loaded TiO_2 surface together with spillover effect [25–31]. At a high temperature (i.e., 350–400°C) (Figure 7(c)), the number of adsorbed oxygen species, particularly O^- or O^{2-}, increased significantly and some of them adsorbed around the Pt nanoparticles. The adsorbed oxygen species will shield Pt particles from H_2 and reduce ability of H_2 dissociation by Pt. Thus, hydrogen response decreases considerably because the spillover effect by Pt is substantially hindered while the rate of direct hydrogen reduction by TiO_2 is still very low. It should be noted that the shielding effect is significant in this case because the Pt particle size of ~2 nm (from TEM data) is only a few times larger than that of oxygen species. The noble metal on the surface of the metal oxide with the role to enrich its surface or the interface with reactive species such as oxygen ions [32, 33]. Therefore, the responsible sensing reaction takes place at the surface of the supporting metal oxide, as shown in Figure 7.

4. Conclusion

In summary, the H_2 sensing process is strongly related to the surface reaction. Different concentrations of noble metal of the highly crystalline unloaded TiO_2 and (0.25, 0.50, 0.75, 1.00, 2.00, and 3.00 mol%) Pt-loaded TiO_2 were synthesized by FSP route. FSP has been shown to be a promising technique for the synthesis of metal oxide and noble loaded-metal oxide in a single step. The structure and morphology of as-prepared products were characterized by HRTEM, SEM, and XRD. Pt-loaded TiO_2 composite particles were deposited on sensor electrode by spin-coating technique. It can be concluded that the fast responses and highest sensor response to H_2 gas were obtained by the incorporation at the optimal 2.00 mol% Pt-loaded TiO_2 at 300°C (to 1 vol%, $S = 470$). The enhanced sensor performance of the Pt-loaded TiO_2 sensors can be attributed to spillover effect, which is most effective at optimally dispersed Pt loading level of 2.00 mol% and moderate operating temperature of 300°C.

Acknowledgments

This research was supported by Thailand's Office of the Higher Education Commission, Uttaradit Rajabhat University; Graduate school, Chiang Mai University; the National Research University Project under Thailand's Office of the Higher Education Commission, Department of Chemistry, Faculty of Science, Chiang Mai University; National Electronics and Computer Technology Center, Pathumthani, Thailand, which are gratefully acknowledged.

References

[1] N. Wetchakun and S. Phanichphant, "Effect of temperature on the degree of anatase-rutile transformation in titanium dioxide nanoparticles synthesized by the modified sol-gel method," *Current Applied Physics*, vol. 8, no. 3-4, pp. 343–346, 2008.

[2] S. Oh, S. Kim, J. E. Lee, T. Ishigaki, and D. Park, "Effect of additives on photocatalytic activity of titanium dioxide powders synthesized by thermal plasma," *Thin Solid Films*, vol. 435, no. 1-2, pp. 252–258, 2003.

[3] J. Jiang, Q. Gao, and Z. Chen, "Gold nanocatalysts supported on protonic titanate nanotubes and titania nanocrystals," *Journal of Molecular Catalysis A*, vol. 280, no. 1-2, pp. 233–239, 2008.

[4] N. Tamaekong, C. Liewhiran, A. Wisitsoraat, and S. Phanichphant, "Acetylene sensor based on Pt/ZnO thick films as prepared by flame spray pyrolysis," *Sensors and Actuators B*, vol. 152, no. 2, pp. 155–161, 2011.

[5] K. Hieda, T. Hyodo, Y. Shimizu, and M. Egashira, "Preparation of porous tin dioxide powder by ultrasonic spray pyrolysis and their application to sensor materials," *Sensors and Actuators B*, vol. 133, no. 1, pp. 144–150, 2008.

[6] V. Brinzari, G. Korotcenkov, and V. Golovanov, "Factors influencing the gas sensing characteristics of tin dioxide films deposited by spray pyrolysis: understanding and possibilities of control," *Thin Solid Films*, vol. 391, no. 2, pp. 167–175, 2001.

[7] I. Bilecka, I. Djerdj, and M. Niederberger, "One-minute synthesis of crystalline binary and ternary metal oxide nanoparticles," *Chemical Communications*, vol. 887, no. 7, pp. 886–888, 2008.

[8] V. Tiwari, J. Jiang, V. Sethi, and P. Biswas, "One-step synthesis of noble metal-titanium dioxide nanocomposites in a flame aerosol reactor," *Applied Catalysis A*, vol. 345, no. 2, pp. 241–246, 2008.

[9] W. Chomkitichai, N. Tamaekong, C. Liewhiran, A. Wisitsoraat, S. Sriwichai, and S. Phanichphant, "H_2 sensor based on Au/TiO_2 nanoparticles synthesized by flame spray pyrolysis," *Engineering Journal*, vol. 16, no. 3, pp. 135–142, 2012.

[10] A. Teleki, N. Bjelobrk, and S. E. Pratsinis, "Flame-made Nb- and Cu-doped TiO_2 sensors for CO and ethanol," *Sensors and Actuators B*, vol. 130, no. 1, pp. 449–457, 2008.

[11] M. N. Carcassi and F. Fineschi, "Deflagrations of H_2-air and CH_4-air lean mixtures in a vented multi-compartment environment," *Energy*, vol. 30, no. 8, pp. 1439–1451, 2005.

[12] T. Tsai, J. Huang, K. Lin, W. Hsu, H. Chen, and W. Liu, "Improved hydrogen sensing characteristics of a Pt/SiO_2/GaN Schottky diode," *Sensors and Actuators B*, vol. 129, no. 1, pp. 292–302, 2008.

[13] W. Liu, K. Lin, H. Chen et al., "A new Pt/oxide/In0.49Ga0.51P MOS Schottky diode hydrogen sensor," *IEEE Electron Device Letters*, vol. 23, no. 11, pp. 640–642, 2002.

[14] A. Yamakata, T. Ishibashi, and H. Onishi, "Kinetics of the photocatalytic water-splitting reaction on TiO_2 and Pt/TiO_2 studied by time-resolved infrared absorption spectroscopy," *Journal of Molecular Catalysis A*, vol. 199, no. 1-2, pp. 85–94, 2003.

[15] T. Samerjai, N. Tamaekong, C. Liewhiran, A. Wisitsoraat, A. Tuantranont, and S. Phanichphant, "Selectivity towards H_2 gas by flame-made Pt-loaded WO_3 sensing films," *Sensors and Actuators B*, vol. 157, no. 1, pp. 290–297, 2011.

[16] N. Tamaekong, C. Liewhiran, A. Wisitsoraat, and S. Phanichphant, "Sensing characteristics of flame-spray-made Pt/ZnO thick films as H_2 gas sensor," *Sensors*, vol. 9, no. 9, pp. 6652–6669, 2009.

[17] E. Antolini and F. Cardellini, "Formation of carbon supported PtRu alloys: an XRD analysis," *Journal of Alloys and Compounds*, vol. 315, no. 1-2, pp. 118–122, 2001.

[18] K. Kim, H. Kim, K. Choi, H. Kim, and J. Lee, "ZnO hierarchical nanostructures grown at room temperature and their C_2H_5OH sensor applications," *Sensors and Actuators B*, vol. 155, no. 2, pp. 745–751, 2011.

[19] M. Seo, M. Yuasa, T. Kida et al., "Gas sensor using noble metal-loaded TiO_2 nanotubes for detection of large-sized volatile organic compounds," *Journal of the Ceramic Society of Japan*, vol. 119, no. 1395, pp. 884–889, 2011.

[20] D. Buso, M. Post, C. Cantalini, P. Mulvaney, and A. Martucci, "Gold nanoparticle-doped TiO_2 semiconductor thin films: gas sensing properties," *Advanced Functional Materials*, vol. 18, no. 23, pp. 3843–3849, 2008.

[21] S. Okazaki, H. Nakagawa, S. Asakura et al., "Sensing characteristics of an optical fiber sensor for hydrogen leak," *Sensors and Actuators B*, vol. 93, no. 1–3, pp. 142–147, 2003.

[22] J. Wöllenstein, H. Böttner, M. Jaegle, W. J. Becker, and E. Wagner, "Material properties and the influence of metallic catalysts at the surface of highly dense SnO_2 films," *Sensors and Actuators B*, vol. 70, no. 1–3, pp. 196–202, 2000.

[23] C. Han, D. Hong, I. Kim, J. Gwak, S. Han, and K. C. Singh, "Synthesis of Pd or Pt/titanate nanotube and its application to catalytic type hydrogen gas sensor," *Sensors and Actuators B*, vol. 128, no. 1, pp. 320–325, 2007.

[24] S. Trocino, A. Donato, M. Latino, N. Donato, S. G. Leonardi, and G. Neri, "Pt-TiO_2/MWCNTs hybrid composites for monitoring low hydrogen concentrations in air," *Sensors*, vol. 12, no. 9, pp. 12361–12373, 2012.

[25] K. Wetchakun, T. Samerjai, N. Tamaekong et al., "Semiconducting metal oxides as sensors for environmentally hazardous gases," *Sensors and Actuators B*, vol. 160, no. 1, pp. 580–591, 2011.

[26] Y. Shimizu, F. Lin, Y. Takao, and M. Egashira, "Zinc oxide varistor gas sensors: II, effect of chromium(III) oxide and yttrium oxide additives on the hydrogen-sensing properties," *Journal of the American Ceramic Society*, vol. 81, no. 6, pp. 1633–1643, 1998.

[27] A. A. Haidry, P. Schlosser, P. Durina et al., "Hydrogen gas sensors based on nanocrystalline TiO_2 thin films," *Central European Journal of Physics*, vol. 9, no. 5, pp. 1351–1356, 2011.

[28] T. Samerjai, N. Tamaekong, K. Wetchakun et al., "Flame-spray-made metal-loaded semiconducting metal oxides thick films for flammable gas sensing," *Sensors and Actuators B*, vol. 171, pp. 43–61, 2012.

[29] M. R. Mohammadi, D. J. Fray, and M. C. Cordero-Cabrera, "Sensor performance of nanostructured TiO_2 thin films derived from particulate sol-gel route and polymeric fugitive agents," *Sensors and Actuators B*, vol. 124, no. 1, pp. 74–83, 2007.

[30] M. Hübner, D. Koziej, J.-D. Grunwaldt, U. Weimar, and N. Barsan, "An Au clusters related spill-over sensitization mechanism in SnO_2-based gas sensors identified by operando HERFD-XAS, work function changes, DC resistance and catalytic conversion studies," *Physical Chemistry Chemical Physics*, vol. 14, no. 38, pp. 13249–13254, 2012.

[31] C. Liewhiran, N. Tamaekong, A. Wisitsoraat, and S. Phanichphant, "H_2 sensing response of flame-spray-made Ru/SnO_2 thick films fabricated from spin-coated nanoparticles," *Sensors*, vol. 9, no. 11, pp. 8996–9010, 2009.

[32] R. S. Niranjan, Y. K. Hwang, D.-K. Kim, S. H. Jhung, J.-S. Chang, and I. S. Mulla, "Nanostructured tin oxide: synthesis and gas-sensing properties," *Materials Chemistry and Physics*, vol. 92, no. 2-3, pp. 384–388, 2005.

[33] C. Wang, L. Yin, L. Zhang, D. Xiang, and R. Gao, "Metal oxide gas sensors: sensitivity and influencing factors," *Sensors*, vol. 10, no. 3, pp. 2088–2106, 2010.